Journal of Solid State Chemistry **161,** 197–204 (2001)
doi:10.1006/jssc.2001.9292, available online at http://www.idealibrary.com on IDEAL®

Structural Distortion and Chemical Bonding in $TlFeO_3$: Comparison with $AFeO_3$ (A = Rare Earth)

Seung-Joo Kim,* Gérard Demazeau,*,[1] Igor Presniakov,† and Jin-Ho Choy‡

*Institut de Chimie de la Matière Condensée de Bordeaux (ICMCB), UPR-CNRS 9048, 87 Avenue de Dr. A. Schweitzer, 33608 Pessac Cedex, France; †Department of Chemistry–Chair of Radiochemistry, Lomonosov Moscow State University, 119899 Moscow V-234, Russia; and ‡National Nanohybrid Materials Laboratory, School of Chemistry and Molecular Engineering, Seoul National University, Seoul 151-747, Korea

Received February 15, 2001; in revised form June 26, 2001; accepted July 2, 2001

The crystal structure and the magnetic properties for thallium orthoferrite, $TlFeO_3$, were characterized and compared with those of rare earth orthoferrites, $AFeO_3$ (A = rare earth). $TlFeO_3$ has a $GdFeO_3$-type perovskite structure (a = 5.3172(2) Å, b = 5.4465(2) Å, and c = 7.7927(3) Å; space group, *Pbnm*). Its cell parameters and unit-cell volume considerably deviate from a trend observed in the rare earth orthoferrites, which are attributed to a specific coordination of Tl^{3+} ion. According to magnetization measurements, $TlFeO_3$ shows an antiferromagnetic behavior accompanied with weak ferromagnetism. The magnetic ordering temperature, T_N (560 K), for $TlFeO_3$ is lower than that for any other orthoferrite while the Fe–O–Fe superexchange angle (144.0°) in $TlFeO_3$ is comparable to that in $ErFeO_3$. The Mössbauer spectrum reveals a single Fe^{3+} quadrupole doublet with an isomer shift $\delta = 0.18 \pm 0.02$ mm/s and a quadrupole splitting value $\Delta = 0.47 \pm 0.02$ mm/s at 623 K ($> T_N$), whereas it shows a magnetic hyperfine sextet with $\delta = 0.47$ mm/s and a hyperfine field $H_{hf}(Fe^{3+}) = 535$ kOe at 80 K ($< T_N$). The magnetism and the Mössbauer results underline a significant competing effect of the Tl–O bond with the covalency of the Fe–O one. Despite the anomalous character of $TlFeO_3$ in structure and magnetism, it is found that the T_N values for all orthoferrites, including $TlFeO_3$, are strongly correlated with their crystallographic axial ratio, $c/\sqrt{2}a$. Through this type of analysis, the electronic effects of A cation on structural distortion and magnetic behavior in perovskite are discussed. © 2001 Academic Press

Key Words: **$TlFeO_3$; orthoferrite; perovskite; structural distortion; magnetism; Mössbauer spectroscopy.**

INTRODUCTION

The perovskites (ABO_3) have attracted considerable interest due to their wide variation of composition and physicochemical properties. In the ideal perovskite structure, which belongs to the cubic space group $Pm\bar{3}m$, the A cation is surrounded by 12 oxygen ions in a regular dodecahedral environment and the B cation is octahedrally coordinated by 6 oxygen ions, giving arise to a 180° B–O–B bond angle. Distortion from the ideal structure is largely related to a mismatch between A–O and B–O bond distances. If the A cation is replaced by a smaller one, BO_6 octahedra would rotate about the cubic crystallographic axis to release the structural stress. The cooperative rotation of BO_6 octahedra consequently leads a decrease in the B–O–B bond angle and a reduction in the coordination number of A cations. Such distortions, controlled by different A cations for the same B cation, play crucial roles in metal–insulator transition (1–3), magnetoresistance (4), spin transition (5, 6), etc., because the electronic structure in perovskite is strongly associated with B–O–B bond angles.

The series of orthoferrites $AFeO_3$, where A is rare earth, have well illustrated (i) how the A cation induces the lattice distortion in perovskite structure and (ii) how the resulting distortion affects magnetic properties. The rare earth orthoferrites crystallize in the orthorhombic perovskite structure (space group, *Pbnm*), which is a common arrangement for many ABO_3 compounds. In early works, Marezio *et al.* (7) showed an evolution of the oxygen coordination around rare earth ions across the series from $PrFeO_3$ to $LuFeO_3$ and proposed that the coordination to first-nearest neighbors varies approximately from 9 (A = Pr) to 8 (A = Nd ~ Tb) and successively to 6 (A = Dy ~ Lu). The orthoferrites are essentially antiferromagnetic with a weak ferromagnetic component (8). The evolution of the magnetic ordering temperature, T_N, values for these oxides has been explained by the Fe–O–Fe superexchange interaction alone, since rare earth ions are still paramagnetic below T_N. On the basis of such investigations, some empirical relations between the T_N and the Fe–O–Fe bond angle governed by the size of the A cation have been suggested (9, 10).

Recently we have prepared an orthonickelate containing Tl^{3+}, $TlNiO_3$ (11), which exhibits a structure distinct from

[1] To whom correspondence should be addressed. E-mail: demazeau@icmcb.u-bordeaux.fr. Fax: 33-(0)5-56-84-27-10.

0022-4596/01 $35.00

that of other $ANiO_3$ (A = rare earth). Its T_N is considerably lower than the value estimated from the Ni–O–Ni bond angle. It has been suggested that the strong covalency of the Tl–O bond, due to the electronic configuration ($[Xe]4f^{14}5d^{10}6s^0$) of Tl^{3+}, could also play an important role in determining the structural and magnetic properties. To confirm such a phenomenon, we would extend this study of $TlFeO_3$. Although the first preparation of $TlFeO_3$ was achieved very early (12), the details of structure and magnetism of this compound were not known.

In this work, $TlFeO_3$ was synthesized under high-pressure conditions and characterized by means of X-ray diffraction, magnetization measurement, and ^{57}Fe Mössbauer spectroscopy. We present the electronic effects of A cations on structure and magnetism for orthoferrites and also discuss the global correlation between lattice distortion and T_N.

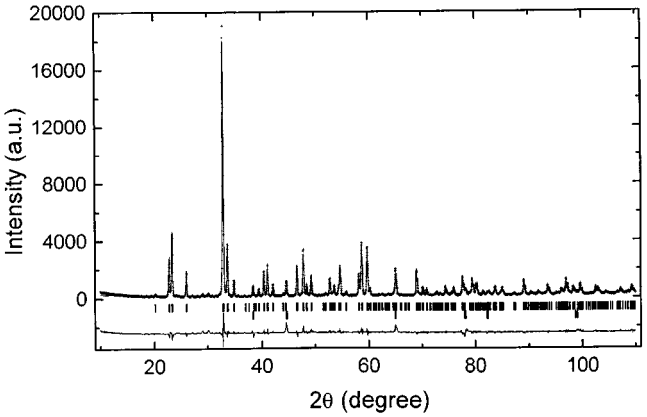

FIG. 1. Observed (crosses), calculated (full line), and difference (bottom) powder X-ray Rietveld profiles for $TlFeO_3$ at room temperature. The upper and lower vertical tick marks show the Bragg positions for $TlFeO_3$ and Al (sample holder).

EXPERIMENTAL

A polycrystalline $TlFeO_3$ sample was prepared under high pressure–high temperature (HP–HT) conditions with a "belt" type apparatus. The stoichiometric amount of Tl_2O_3 and Fe_2O_3 was thoroughly mixed and encapsulated in a gold tube with a diameter of 3 mm. The capsule was separated by NaCl powder from a graphite tube (internal heater) before being heated and 850°C under 7 GPa for 30 min (12).

Powder X-ray diffraction profiles were recorded on a Philips PW 1050 diffractometer using graphite-monochromated Cu$K\alpha$ radiation. Data were collected over the 2θ range from 10° to 110° for 4 s in each 0.02° step at ambient temperature. The structural parameters were refined with the Rietveld program FULLPROF (13). The background level was optimized with a polynomial function and the peak shape was fitted to a pseudo-Voïgt function.

The magnetization was measured with a Faraday-type DSM-8 magnetometer in the temperature range from 300 to 750 K at 1.7 T. The magnetic hysteresis was monitored with SQUID (Quantum Design MPMS-5S) at 300 K.

The ^{57}Fe Mössbauer spectra were recorded at 623 and 80 K using a conventional constant-acceleration Mössbauer spectrometer. The radiation source $^{57}Co(Rh)$ was kept at room temperature. All isomer shifts refer to the α-Fe absorber at 300 K.

RESULTS AND DISCUSSION

Crystal Structure of $TlFeO_3$ and Comparison with $AFeO_3$ (A = Rare Earth)

All reflections for $TlFeO_3$ in the powder XRD pattern were indexed by a primitive orthorhombic unit cell (space group = *Pbnm*) with $a = 5.3172(2)$ Å, $b = 5.4465(2)$ Å, and $c = 7.7927(3)$ Å, which are consistent with the previous report (12). The observed, calculated, and difference patterns from Rietveld refinement are shown in Fig. 1. The final atomic coordinates, isotropic temperature factors, and agreement factors are given in Table 1 and the selected bond distances and bond angles are listed in Table 2.

The three Fe–O distances in $TlFeO_3$ are in the range from 1.97 to 2.06 Å. The average Fe–O bond distance is estimated as 2.013 Å, which is in agreement with the Fe^{3+}–O bond distances (2.009–2.014 Å) observed in $AFeO_3$ (A = rare earth) (8). The O–Fe–O angles somewhat deviate from 90°. The oxygen polyhedron around Tl appears to be severely distorted. The twelve Tl–O bond distances vary from 2.225 to 3.381 Å. A view of the $TlFeO_3$ structure is illustrated in Fig. 2.

It is interesting to compare the structural distortion for $TlFeO_3$ with those observed for the isostructural series, $AFeO_3$. The unit-cell parameters (a, b, c) for these compounds are plotted as a function of the radius of the A^{3+} ion (Fig. 3). We adopt the ionic radii (C.N. = 8) proposed by Shannon (14) for a comparison. For all orthoferrites except for $TlFeO_3$, the unit-cell parameters and the unit-cell

TABLE 1
Unit-Cell, Positional, and Thermal Parameters for $TlFeO_3$ in the Orthorhombic *Pbnm* Space Group

$R_{wp} = 10.9\%$, $R_{exp} = 4.67\%$, $R_I = 5.42\%$, $\chi^2 = 5.46$
$a = 5.3172(2)$ Å, $b = 5.4465(2)$ Å, $c = 7.7927(3)$ Å, $Z = 4$

	Site	g	x	y	z	B (Å^2)
Tl	4*c*	1	0.9856(3)	0.0481(2)	0.25	0.53(2)
Fe	4*b*	1	0.5	0	0	0.34(7)
O1	4*c*	1	0.105(2)	0.442(3)	0.25	0.6(2)
O2	8*d*	1	0.694(2)	0.312(3)	0.053(2)	0.6(2)

TABLE 2
Selected Bond Distances and Bond Angles for $TlFeO_3$

	Multiplicity	Bond distance (Å)		Bond angle (°)
Tl–O1^{iv}	1	2.243(16)	O1–Fe–O2	86.8(7)
Tl–O1^{i}	1	2.231(13)	O1–Fe–O2	85.8(6)
Tl–O1^{iii}	1	3.215(12)	O2–Fe–O2	88.4(9)
Tl–O1^{ii}	1	3.365(16)		
Tl–O2^{i}	2	2.225(11)		
Tl–O2^{iii}	2	2.593(11)	Fe–O1–Fe	142.5(2)
Tl–O2^{v}	2	2.737(10)	Fe–O2–Fe	144.7(5)
Tl–O2^{vii}	2	3.381(8)		
Fe–O1	2	2.057(5)		
Fe–O2	2	1.974(11)		
Fe–O2	2	2.019(12)		

volume change systematically with respect to the ionic radius of A^{3+}. Such relations for $AFeO_3$ (A = rare earth) were already investigated in several works. The two unit-cell parameters a and c and the unit-cell volume decrease gradually with decreasing rare earth ion size, while the b parameter is nearly constant. The continuous variations give

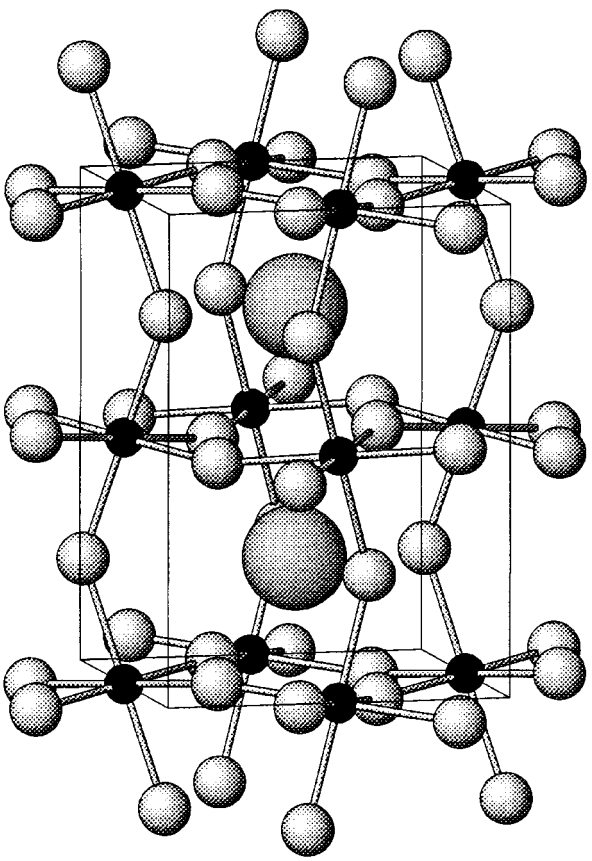

FIG. 2. Crystal structure model of $TlFeO_3$. The c axis is vertical, and the a axis goes from right to left. Large spheres, small dark spheres, and small bright spheres represent Tl, Fe, and O atoms, respectively.

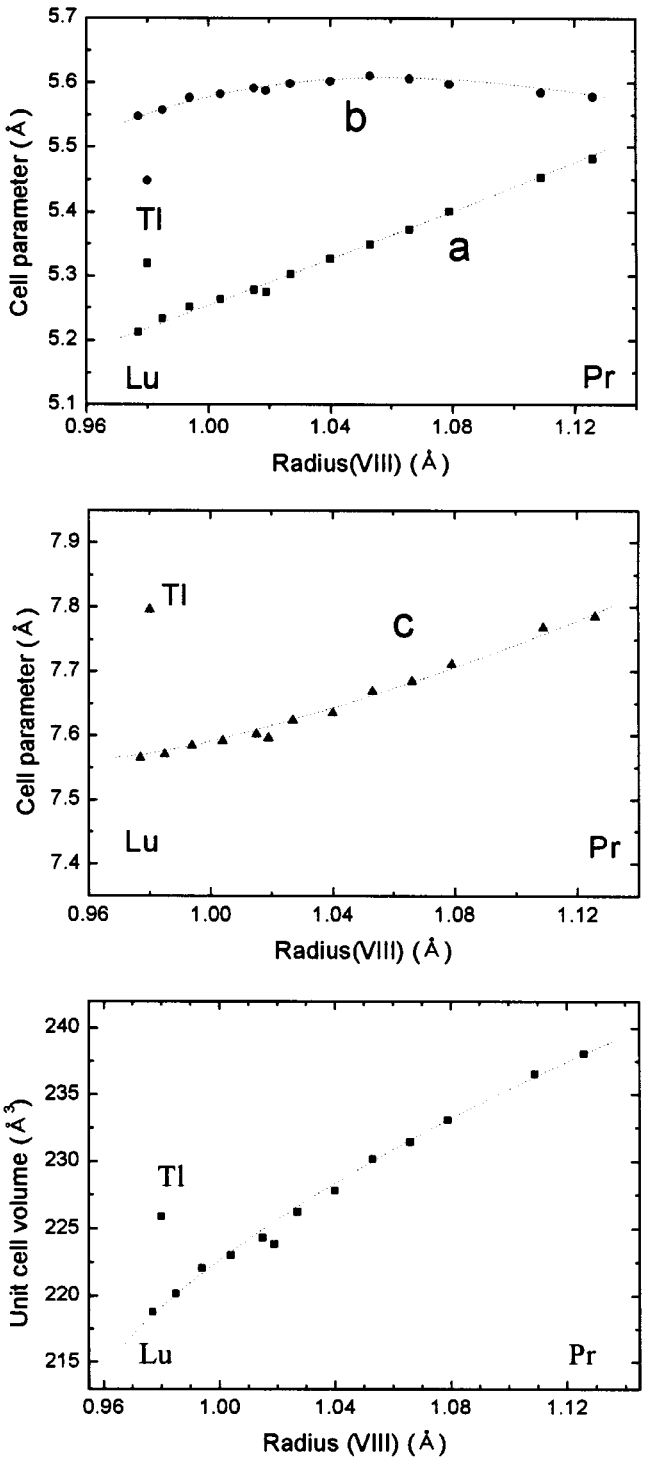

FIG. 3. Relation between the ionic radius of the A cation and the unit-cell parameters (top and middle) and the unit-cell volume (bottom) for $TlFeO_3$ and $AFeO_3$ (7) (A = rare earth).

interpolated curves allowing us to predict the lattice distortion for the corresponding compound. However, a, b, and c for $TlFeO_3$ deviate from these curves by -0.11, $+0.09$, and $+0.22$ Å, respectively. In particular, the c for $TlFeO_3$ is

larger than that for $PrFeO_3$ although the Tl^{3+} ion is much smaller than the Pr^{3+} one. As a consequence, $TlFeO_3$ has a large unit-cell volume (225.91 $Å^3$), which is comparable to that of $DyFeO_3$, deviated from the relation between the unit-cell volume and the ionic radius of the A cation for $AFeO_3$.

To understand such an anomalous structural character for $TlFeO_3$, we compared the Tl–O bond distances with the A–O ones in the orthoferrites. In an ideal perovskite structure, the A cation is coordinated by 12 equidistant oxygen ions. If the A cation is substituted with a smaller one, the $\langle AO_{12}\rangle$ dodecahedron is distorted, leading to a change in the distribution of the A–O bond distances. In $GdFeO_3$ type structure, it has been well known that 8 A–O bonds among the 12 bonds become shorter and the other 4 A–O bonds become longer gradually as the size of the A cation decreases. This trend is obvious for the compounds from $NdFeO_3$ to $TbFeO_3$ for which the A cation is coordinated with 8 oxygen ions as the first-nearest neighbors and 4 oxygen ions as the second-nearest neighbors. The coordination number of the A cation, consequently, can be expressed as $8 + 4$ for these examples. When proceeding from $DyFeO_3$ to $LuFeO_3$, the distances from the rare earth to 7th and 8th oxygen ions slightly increase so that the corresponding oxygen ions become second-nearest neighbors as described in earlier work (7). $TlFeO_3$, however, shows a different distribution of Tl–O bond distances. The 5th and 7th Tl–O bond distances, i.e., d(Tl–O2^{iii}) and d(Tl–O2^{v}), are considerably larger than the corresponding A–O bond distances in $AFeO_3$, which is directly related to the large c parameter of $TlFeO_3$. As a result, the 12 Tl–O bond distances can be grouped into three groups: (i) 4 short bonds with 2.225–2.243 Å, (ii) 4 intermediate bonds with 2.593–2.737 Å, and (iii) 4 long bonds with 3.215–3.381 Å. The coordination number of Tl^{3+}, therefore, could be expressed as $4 + 4 + 4$ approximately (Fig. 4). Such a behavior is very similar to that for $TlNiO_3$ where there groups of Tl–O distances were also observed (11). The specific environment around the Tl^{3+} ion may be attributed to the electronic configuration of the Tl^{3+} ion. The post-transition metal ion Tl^{3+} is more polarizing due to its fully occupied 4f and 5d orbital ([Xe]4$f^{14}5d^{10}6s^0$), leading to a bond to oxygen more covalent than that of rare earth ions. The strong covalent character of the Tl–O bond probably induces a directional effect and allows the Tl^{3+} ion to have such a specific coordinated environment distinguished from rare earth ions, which results in the large unit-cell volume.

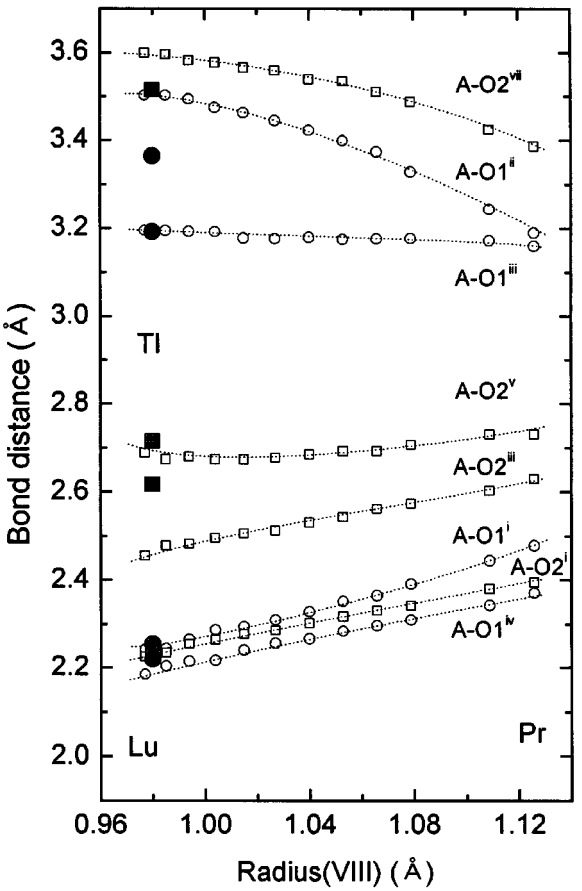

FIG. 4. Variation of the A–O bond distances on the ionic radius of the A cation in the orthoferrites. ○, □, ●, and ■ represent the A–O1, A–O2, Tl–O1, and Tl–O2 bond distances, respectively. The multiplicities of A(Tl)–O1 and A(Tl)–O2 are 1 and 2, respectively. The bond distances for $AFeO_3$ (A = rare earth) are plotted on the basis of values in Ref. 7.

Magnetic Property of $TlFeO_3$

The temperature dependence of magnetization for an applied magnetic field of 1.7 T shows an abrupt change around 560 K (Fig. 5). Above this temperature, the magnetism follows a Curie–Weiss behavior and then the corresponding effective magnetic moment, μ_{eff}, is estimated as 6.5 μ_B, which is close to the spin-only value (5.9 μ_B) for high spin Fe^{3+}. The Weiss constant, θ_w, and the ratio θ_w/T_c are -1200 K and 2.1 respectively. The magnetization versus applied field at 300 K exhibits a hysteresis loop. Starting from high field the magnetization decreases linearly with field to 0 T around which it falls abruptly and then it gradually follows the linear behavior in the opposite field direction and *vice versa* (Fig. 6). A weak magnetization of 70 emu/mol is maintained at zero field. Such magnetic behavior has been observed in all the rare earth orthoferrites where the small ferromagnetic moment is due to a slight canting of magnetic moment from the direction of their antiferromagnetic vector. This magnetic structure has been described by a result of Dzyaloshinsky's antisymmetric superexchange (15). The canting angle is estimated at 8–10 mrad ($\sim 0.5°$) for rare earth orthoferrites. The magnetism of $TlFeO_3$, consequently, can be characterized as an antiferromagnetism with $T_N = 560$ K accompanied with

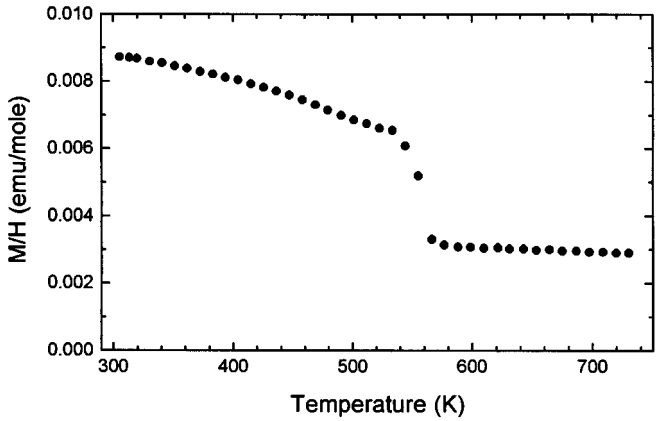

FIG. 5. Temperature dependence of the magnetization M/H for $TlFeO_3$ at constant field strength of 1.7 T.

a weak ferromagnetism. The spontaneous magnetization corresponds to 0.016 μ_B/mol, which is somewhat smaller than the spontaneous magnetizations (0.03–0.07 μ_B/mol) of other orthoferrites (10).

Structural Distortion and Magnetism

An empirical relation (10) between the magnetic ordering temperature, T_N, and the Fe–O–Fe bond angle, φ, in rare earth orthoferrites, $AFeO_3$ (Fig. 7a) has been suggested:

$$T_N \propto \cos^2 \varphi.$$

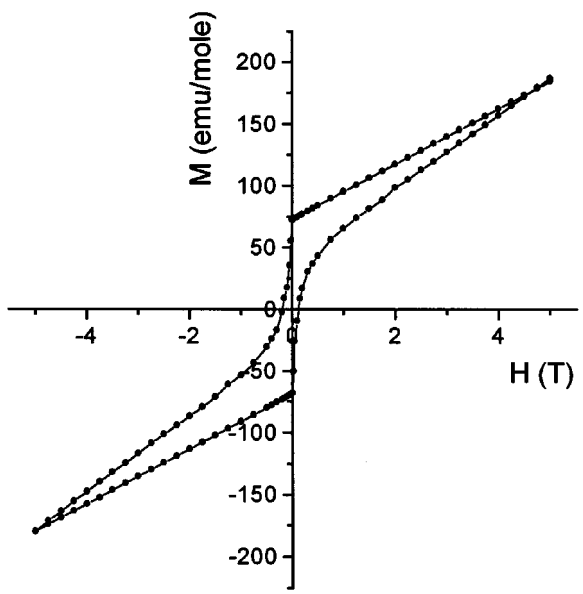

FIG. 6. Hysteresis loop at 300 K for $TlFeO_3$.

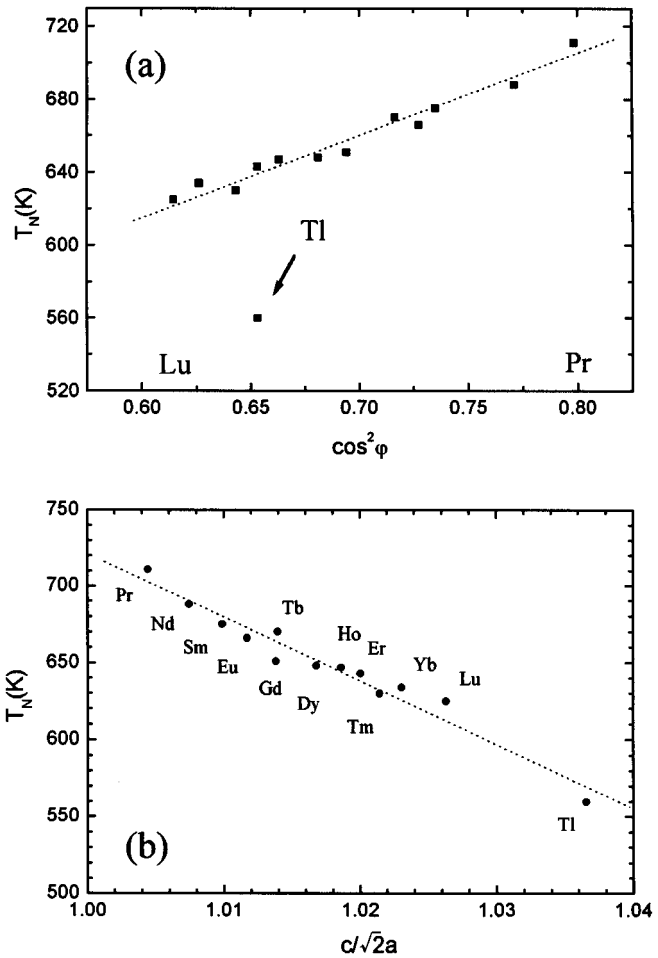

FIG. 7. Evolution of T_N on (a) Fe–O–Fe superexchange angle and (b) crystallographic axial ratio, $c/\sqrt{2}a$, for orthoferrites.

However, $TlFeO_3$ shows a significant deviation from this relation. Although the Fe–O–Fe bond angle, φ, for $TlFeO_3$ is close to 144.0°, which is comparable to that for $ErFeO_3$, the T_N (560 K) for $TlFeO_3$ is much lower than that for $ErFeO_3$ (643 K). The difference in T_N for both compounds with the similar superexchange angles may be explained by different characteristics of two chemical bonds, Tl–O and Er–O. The strong Tl–O bond, competing with the Fe–O one for electron density on oxygen, may weaken the interaction between Fe^{3+} ions via oxygen. However, it is difficult to estimate quantitatively the bond strength by a method such as *XRD* because the variation in the Fe–O bond distance governed by the change in A cation is quite small. The Fe–O bond distance varies within the range of 0.005 Å across the series of rare earth orthoferrites, $AFeO_3$.

It should be noted that the competition of the A–O bond and the B–O bond could be estimated from the relation between the lattice distortion and the magnetic ordering temperature. According to Glazer's tilt system (16), the

$GdFeO_3$ type perovskite structure is described by an octahedral tilting type, $a^0b^+c^+$, in an orthorhombic system. (The $a^0b^+c^+$ tilting type in the orthorhombic system corresponds to the $a^+b^-b^-$ type in the pseudocubic system. The former notation means that two kinds of tilts of the octahedra about [010] and [001] orthorhombic axes are combined with each other. The + sign means that the tilts are in phase when successive octahedra along the same axis are considered (Fig. 2). The two tilts have different magnitudes represented by b and c.) The variations of the unit-cell parameters are related with the magnitudes of the tilts b and c. If the in-phase tilt about [010] axis b increases, the unit-cell parameters a and c would decrease. If the in-phase tilt about [001] axis c increases, the unit-cell parameter a would decrease and b would increase while c would remain unchanged. Therefore a ratio of the cell parameters, $c/\sqrt{2}a$, could give information about the overall structural distortion as a combination of these two kinds of tilts. In Fig. 7b, it is found that $c/\sqrt{2}a$ increases gradually going from $PrFeO_3$ to $LuFeO_3$ and the value is largest for $TlFeO_3$ despite the relatively large Tl^{3+} ionic size. This fact cannot be explained by the A cation size alone. Moreover, a clear relation between the T_N values and the corresponding ratio, $c/\sqrt{2}a$, is found for the various orthoferrites. T_N for all orthoferrites including $TlFeO_3$ decreases with increasing values of $c/\sqrt{2}a$, all the points of T_N falling on a line within an error limit of 10 K.

Why does the ratio $c/\sqrt{2}a$ reflect the T_N value? It may be related to electronic density around the A cation. Through synchrotron X-ray study for rare earth compounds including La^{3+}, Gd^{3+}, and Lu^{3+} with closed subshell cores, Chatterjee *et al.* (17) indicated that the spherical symmetry of the orbitals for these elements is not preserved when the atoms bind, but the electron cloud is polarized along a specific direction. The highly polarized electron density of the A cation was observed in several rare earth orthoferrites, $AFeO_3$ (A = Y (18), Nd, Dy (19)), which is due to the proximity of the rare earth unfilled d and f states to their filled states. As the atomic number increases, the energy gap to neighboring levels decreases so that the electron density is significantly affected (20). That the $c/\sqrt{2}a$ value for $TlFeO_3$ is much larger than the values observed for other $AFeO_3$ implies the strong polarizability of the Tl–O bond due to the small energy gap between the filled 5d orbital and the empty 6s one of Tl^{3+}, which is also related to the strong covalency of the Tl–O bond. The dependence of T_N on $c/\sqrt{2}a$ shows how the nature of the A cation affects the Fe–O bond in perovskite structure. The strong polarizability of the Tl–O bond induces an elongation of the unit cell with the direction perpendicular to the mirror plan in the orthorhombic perovskite structure. It could also contribute to decreased Fe–O bond strength, leading to low T_N values for $TlFeO_3$ despite a relatively large Fe–O–Fe superexchange angle, φ (144°), compared to those for rare earth orthoferrites (142°–153°). The correlation between $c/\sqrt{2}a$ and T_N may be applicable to a variety of other perovskite series.

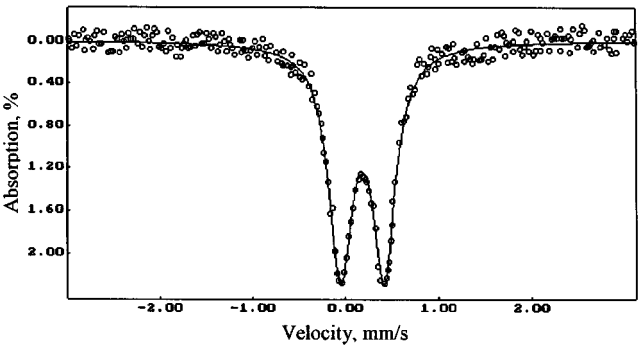

FIG. 8. ^{57}Fe Mössbauer spectrum of $TlFeO_3$ at 623 K ($T > T_N$).

Mössbauer Spectroscopy

The ^{57}Fe Mössbauer spectrum recorded at 623 K ($> T_N$) can be described as a symmetric quadrupole doublet (Fig. 8) with an isomer shift $\delta = 0.18 \pm 0.02$ mm/s, characteristic of Fe^{3+} ions in a high spin state in octahedral coordination (21). The full linewidth at half-height for each component of this doublet ($\Gamma = 0.27 \pm 0.01$ mm/s) was found to be close to the correspondent value for the calibration spectra ($\Gamma = 0.24$ mm/s), which is evidence for crystallographically equivalent positions of Fe^{3+} cations. The quadrupole splitting value ($\Delta = 0.47 \pm 0.02$ mm/s) is an order of magnitude larger than those for the rare earth orthoferrites $AFeO_3$ where only a slight broadening of the Mössbauer line is observed above T_N (22). Since the Fe^{3+} cations in the high spin state have the isotropic electronic configuration $3d^5$ ($t_{2g}{}^3e_g^2$, $^6A_{1g}$), the electric field gradient (EFG) observed at the $^{57}Fe^{3+}$ nuclei is due to the distortion of their crystallographic surroundings (lattice contribution). Therefore, the large value of the quadrupole doublet splitting is evidence for a considerable distortion of the nearest anionic environment that is apparent from the Fe–O distances in X-ray diffraction study (Table 2). To correlate the experimental values with the crystallographic structure, we attempted to theoretically determine the magnitude of the principal EFG components at Fe^{3+} cations in $TlFeO_3$.

Calculations were performed in terms of the "ionic" model, including monopole and dipole contributions of all the ions with the charges coinciding with their formal oxidation states. The EFG tensor components (V_{ij}) were calculated by the equations

$$V_{ij}^{m} = \sum_k Z_k(3x_{ik}x_{jk} - \delta_{ij}r_k^2)r_k^{-5};$$

and

$$V_{ij}^{d} = \sum_{k} -3 \cdot [(x_{ik}p_{ik})(5x_{ik}x_{jk} - \delta_{ij}r_k^2)r_k^{-7} - (p_{ik}x_{ik} + p_{jk}x_{ik})r_k^{-5}],$$

where V_{ij}^{m} and V_{ij}^{d} are the monopole and dipole contributions to the EFG tenzor, Z_k is the effective charge, x_{ik} and x_{jk} are the Cartesian coordinates of the kth ion at the distance r_k from the origin, and δ_{ij} is the Kronecker index. The ith component of the induced dipole moment on the kth ion (p_{ik}) was calculated by the equation

$$p_{ik} = \sum_{j} \alpha_{ij}^{k} E_j^k$$

(α_{ij}^k and E_j^k are the components of the polarizability tensor and the electric field vector, respectively) with the use of a self-consistent iterative procedure. As follows from the local symmetry of the crystallographic sites of the ions in $TlFeO_3$, only the oxygen anions contribute to V_{ij}^{d}. The choice of the value of the dipole polarizability of oxygen (α_O) is a complicated problem (23). This value is not well known and is usually estimated from the best fit of the theoretical EFGs to the measured data. In our calculations we used values of α_O in the range 0.1–2.0 Å^3. The calculated EFG tensors were diagonalized, and the principal values of $V_{\alpha\alpha}$ were designated according to the usual convention $|V_{zz}| > V_{yy}| > |V_{xx}|$; $q^{(1)} = V_{zz}/|e|$ and $\eta = V_{xx} - V_{yy}/V_{zz}$ ($0 \le \eta \le 1$) were selected as independent parameters. A comparison of the calculated $q^{(1)}$ and η values with the corresponding experimental data was performed with the use of the expression that relates the quadrupole splitting (Δ) at $T > T_N$ to the crystallographic and nuclear parameters of the Mössbauer atom,

$$\Delta = (1 - \gamma_\infty)\frac{e^2qQ}{2}(1 + \eta^2/3)^{1/2},$$

where Q (0.082 barn) (24) is the quadrupole moment of the ^{57}Fe nucleus in the first excitation state; γ_∞ (−9.14) (25) is the Sternheimer antishielding factor, which accounts for the distortion of the Fe^{3+} electron core induced by surrounding ions; and η is the EFG asymmetry parameter.

The calculated $q^{(1)}$ and η values are in the range from $q^{(1)} = -0.12$ Å^{-3} and $\eta = 0.93$ (for $\alpha_O = 0.1$ Å^3) to $q^{(1)} = -0.39$ Å^{-3} and $\eta = 0.51$ (for $\alpha_O = 2.0$ Å^3). Substituting the $q^{(1)}$ and η values in the above expression for quadrupole splitting, we obtain the value of $\Delta_{(theor)}$ in the range 0.16–0.49 mm/s. Best agreement with experimental Δ value is obtained with the value $\alpha_O = 1.9$ Å^3 ($q = -0.37$ Å^{-3}; $\eta = 0.50$), which is in accordance with those observed in most ionic oxides (23). This result is rather surprising since in our calculations we used the simple model that presumes the ionic character of chemical bonding; this simplification leads to uncertainty in choosing the effective charges Z_k on the ions. Besides, it was shown that in oxides a significant contribution ($q^{(ov)}$) to the EFG arises from covalency and overlap distortion of the closed metal orbitals by surrounding ligand orbitals (26). In this respect, a good agreement between the $\Delta_{(theor)}$ value calculated form the ionic point–multipole model and Δ obtained from Mössbauer spectra confirms the increased ionic character of the Fe^{3+}–O bonds in $TlFeO_3$. Nevertheless, it should be noted that precise calculations cannot be made as long as accurate values for the electornic polarizability are not available.

In the absence of any structural phase transition, as in our case for $TlFeO_3$, the lattice contribution of the EFG ($q^{(1)}$) is nearly independent of the temperature. This fact allowed us to use the quadrupole coupling constant $e^2q^{(1)}Q$ ($=2\Delta$) obtained from the spectra recorded at $T > T_N$ for calculating the hyperfine structure parameters corresponding to combined magnetic and quadrupole interactions at $T < T_N$.

The ^{57}Fe Mössbauer spectrum recorded at 80 K, i.e., at $T \ll T_N$, consists of one hyperfine splitting pattern reflecting combined quadrupole and magnetic interactions (Fig. 9). When the quadrupole interaction is much smaller than the magnetic interaction in a magnetically split spectrum the shift in the line positions due to the quadrupole interaction is given by

$$\varepsilon_Q = e^3q^{(1)}Q \cdot (3\cos^2\theta - 1)/8,$$

where θ is the angle between $q^{(1)}$ and the direction of the hyperfine field (H_{hf}) at the iron site. The analysis of the spectrum, with fixed $|e^2q^{(1)}Q| = 0.94$ mm/s, enables one to determine the sign of the quadrupole coupling constant $e^2q^{(1)}Q < 0$ and the polar angle $\theta = 46 \pm 5^\circ$. Since the quadrupole moment Q of the first excited state of ^{57}Fe is known to be positive (24), the negative value of $e^2q^{(1)}Q$ means that the main component, $q^{(1)}$, of EFG is also negative. The resulting negative sign for $q^{(1)}$ is in accordance with our calculations of the $q^{(1)}$ value and, consequently, with the local crystallographic structure of $TlFeO_3$ where tetragonally distorted polyhedra FeO_6 are characterized by four short Fe–O distances in the basal plane ($\langle R_\perp \rangle \approx 1.99$ Å) and two elongated bonds ($\langle R_\parallel \rangle \approx 2.06$ Å, Table 2) along the local fourfold axis, which is nearly coincident with the direction of the EFG at the Fe^{3+} nucleus. The θ value is in good agreement with the 45° value found in $BiFeO_3$, having an unusual spiral magnetic structure (27). However, no magnetic data exist for $TlFeO_3$, which precludes conclusions to be drawn concerning the relationship between the θ value and the magnetic structure of the local surroundings of Fe^{3+} ions in the $TlFeO_3$.

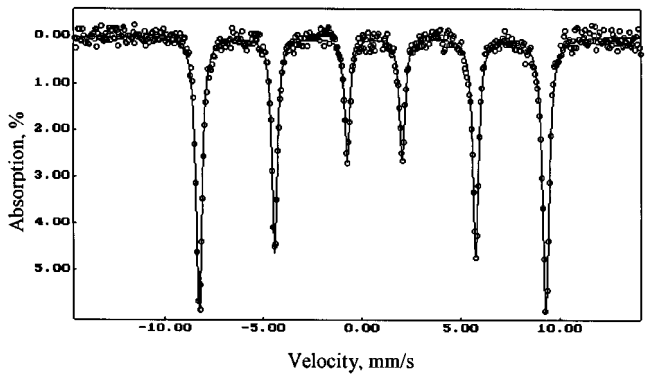

FIG. 9. ^{57}Fe Mössbauer spectrum of $TlFeO_3$ at 80 K ($T > T_N$).

The isomer shift value $\delta = 0.53 \pm 0.02$ mm/s at $T = 80$ K shows the usual increase with respect to the high-temperature value due to the second-order Doppler effect (28). From the theoretical slope $d\delta(T)/dT = 7.3 \times 10^{-4}$ mm/s obtained for a solid below its Debye temperature, an increase of about 0.39 mm/s is expected. This is in good agreement with our observed increase (≈ 0.35 mm/s) over the high-temperature value. The δ value appeared to be somewhat larger than the δ value (0.47 mm/s) at 80 K reported for the rare earth orthoferrites $AFeO_3$ (24). Such a difference is expected from the more pronounced inductive effect of the antagonistic Tl^{3+}–O bonds, which reduce the covalency of the Fe^{3+}–O bonds for $TlFeO_3$ as compared to those in the rare earth orthoferrites $AFeO_3$. This fact is supported by the lower value of the hyperfine field $H_{hf}(Fe^{3+}) = 535$ kOe ($T = 80$ K) at the Fe^{3+} nucleus observed for $TlFeO_3$ compared to the values of the hyperfine field for $AFeO_3$. The various contributions to the hyperfine field have already been discussed extensively in connection with the orthoferrites (29). It has been shown that one of the major contribution to the $H_{hf}(Fe^{3+})$ value is from the supertransferred hyperfine field (H_{sthf}) which is produced by the spins at neighboring Fe^{3+} cations by transfer effect through the intervening anion. Since the H_{sthf} depends on the spin transfer in much the same way as superexchange, we expect that the hyperfine field $H_{hf}(Fe^{3+})$ also strongly depends upon the characteristics (geometry and ionicity) of the Fe–O–Fe bonds. The reduction in $H_{hf}(Fe^{3+})$ value on going from $EuFeO_3$ ($H_{hf} = 550$ kOe at $T = 80$ K) (24) to $TlFeO_3$ ($H_{hf} = 535$ kOe) having the similar Fe–O–Fe superexchange angle ($\approx 144^\circ$) provides further evidence for decreasing Fe^{3+}–O bond strength for $TlFeO_3$ as compared to that for $EuFeO_3$.

CONCLUSION

The anomalous cell parameters and the large unit-cell volume of $TlFeO_3$ are attributed to the specific coordinating environment around the Tl^{3+} ion. The low T_N for $TlFeO_3$ may result from the reduced electron density in the Fe–O bond by the strongly covalent Tl–O bond. Although individual cell parameters for $TlFeO_3$ deviate from the trends observed in other orthoferrites, the ratio $c/\sqrt{2}a$ for all orthoferrites including $TlFeO_3$ shows a linear dependence on T_N, which implies that the lattice distortion is strongly correlated with the polarizing effect of the A cation. In ^{57}Fe Mössbauer spectra, the higher δ value and the lower H_{hf} value observed for $TlFeO_3$ compared to those for $AFeO_3$ orthoferrites confirm the strong inductive effect of the Tl^{3+}–O bond on the Fe^{3+}–O bonds.

REFERENCES

1. G. Demazeau, A. Marbeuf, M. Pouchard, and P. Hagenmuller, *J. Solid State Chem.* **3,** 582 (1971).
2. J. B. Torrance, P. Lacorre, A. I. Nazzal, E. J. Ansaldo, and Ch. Niedermayer, *Phys. Rev. B* **45,** 8209 (1992).
3. J. A. Alonso, M. J. Martínez-Lope, M. T. Casais, J. L. García-Muñoz, and M. T. Fernández-Díaz, *Phys. Rev. B* **61,** 1756 (2000).
4. K. Chahara, T. Ohno, M. Kassai, and Y. Kozono, *Appl. Phys. Lett.* **63,** 1990 (1993).
5. G. Demazeau, M. Pouchard, and P. Hagenmuller, *J. Solid State Chem.* **9,** 202 (1974).
6. S. Yamaguchi, Y. Okimoto, and Y. Tokura, *Phys. Rev. B* **54,** R11022 (1996).
7. M. Marezio, J. P. Remeika, and P. D. Dernier, *Acta Crystallogr. B* **26,** 2008 (1970).
8. D. Treves, *J. Appl. Phys.* **36,** 1033 (1965).
9. K. Motida and S. Miyahara, *J. Phys. Soc. Jpn.* **28,** 1188 (1970).
10. D. Treves, M. Fibchutz, and P. Coppens, *Phys. Lett.* **18,** 126 (1965).
11. S.-J. Kim, G. Demazeau, J. A. Alonso, and J.-H. Choy, *J. Mater. Chem.* **11,** 487 (2001).
12. R. D. Shannon, *Inorg. Chem.* **6,** 1474 (1967).
13. J. Rodriguez-Carvajal, *FULLPROF*, Version 3.2, LLB-CEA, Saclay, France, 1997.
14. R. D. Shannon, *Acta Crystallogr. A* **32,** 751 (1976).
15. I. Dzyaloshinsky, *J. Phys. Chem. Solids* **4,** 241 (1958).
16. A. M. Glazer, *Acta Crystallogr. B* **28,** 3384 (1972).
17. A. Chatterjee, E. N. Maslen, and K. J. Watson, *Acta Crystallogr. B* **44,** 386 (1988).
18. D. du Boulay, E. N. Maslen, and V. A. Streltsov, *Acta Crystallogr. B* **51,** 921 (1995).
19. V. A. Streltsov and N. Ishizawa, *Acta Crystallogr. B* **55,** 1 (1999).
20. J. Blixt, J. Glaser, J. Mink, I. Persson, P. Persson, and M. Sandström, *J. Am. Chem. Soc.* **117,** 5089 (1995).
21. F. Menil, *J. Phys. Chem. Solids* **46,** 763 (1985).
22. M. Eibschütz, S. Shtrikman, and D. Treves, *Phys. Rev.* **156,** 562 (1967).
23. R. Kirsh, A. Gérard, and M. Wautelet, *J. Phys. C: Solid State Phys.* **7,** 3633 (1974).
24. K. J. Duff, K. C. Mishra, and T. P. Das, *Phys. Rev. Lett.* **46,** 1611 (1981).
25. R. M. Sternheimer, *Phys. Rev.* **130,** 1423 (1963).
26. G. A. Sawatzky and F. Van der Woude, *J. Phys. Colloq.* **35,** C6–47 (1974).
27. C. Blaauw and F. Van der Woude, *J. Phys. C: Solid State Phys.* **6,** 1422 (1973).
28. B. D. Josephson, *Phys. Rev. Lett.* **4,** 341 (1960).
29. C. Boekema, F. Van der Woude, and G. A. Sawatzky, *Int. J. Magn.* **3,** 341 (1972).